

New Reaction Pathways for $\mu\text{-}\eta^1, \eta^2\text{-Allenyl Ligands: On–Off Allenyl Coordination and CO Insertion into the Hydrocarbyl Bridge in $\text{Ru}_2(\text{CO})_6(\mu\text{-PPh}_2)\{\mu\text{-}\eta^1, \eta^2_{\alpha, \beta}\text{-C(Ph)=C=CPh}_2\}$$

Peter Blenkiron,[†] John F. Corrigan,[‡] Nicholas J. Taylor,[‡] and Arthur J. Carty*,^{†,‡}

The Steacie Institute for Molecular Sciences, National Research Council of Canada, 100 Sussex Drive, Ottawa, Ontario, Canada K1A 0R6, and Guelph-Waterloo Centre for Graduate Work in Chemistry, Waterloo Campus, Department of Chemistry, University of Waterloo, Waterloo, Ontario, Canada N2L 3G1

Simon Doherty,* Mark R. J. Elsegood, and William Clegg
Department of Chemistry, Bedson Building, University of Newcastle,
Newcastle upon Tyne NE1 7RU, United Kingdom

Received August 21, 1996[Ⓢ]

Summary: The binuclear allenyl complex $\text{Ru}_2(\text{CO})_6(\mu\text{-PPh}_2)\{\mu\text{-}\eta^1, \eta^2_{\alpha, \beta}\text{-C(Ph)=C=CPh}_2\}$ (**1**) reacts with bis-(diphenylphosphino)methane (dppm) to afford $\text{Ru}_2(\text{CO})_4(\mu\text{-PPh}_2)(\mu\text{-dppm})\{\mu\text{-}\eta^1, \eta^2\text{-C(O)C(Ph)=C=CPh}_2\}$ (**2**) containing an acylallenyl ligand and $\text{Ru}_2(\text{CO})_4(\mu\text{-PPh}_2)(\mu\text{-dppm})\{\mu\text{-}\eta^1, \eta^2_{\alpha, \beta}\text{-C(Ph)=C=CPh}_2\}$ (**4**). With bis(diphenylphosphino)ethane (dppe), **1** affords $\text{Ru}_2(\text{CO})_5(\mu\text{-PPh}_2)(\eta^2\text{-dppe})\{\eta^1\text{-C(Ph)=C=CPh}_2\}$ (**3**), which contains a terminal η^1 -coordinated allenyl fragment. The X-ray structures of **2–4** are reported.

The reactivity of the cumulated C_3 hydrocarbyl group $-\text{C(R)=C=CR}'_2$ (allenyl) has been much less extensively developed than that of unsaturated C_2 groups (e.g., alkynyl and alkenyl). Several recent developments suggest that mono- and polynuclear allenyl complexes undergo a variety of novel transformations which herald the beginning of an exciting organometallic chemistry for this fragment.¹ Examples include η^1 - to η^3 -bonding changes at a mononuclear center,² the generation of dimetallocyclopentanes and pentenes via nucleophilic attack at C_β ³ in $\mu\text{-}\eta^1, \eta^2_{\alpha, \beta}$ -allenyl complexes,⁴ azatrimethylenemethanes from C_β addition of amines in η^3 -platinum complexes,⁵ cycloaddition and coupling reactions with dienophiles and alkynes,⁶ the mutual isomerization of (η^1 -allenyl)- and (η^1 -propargyl)platinum complexes,⁷ new ligand coupling/insertion reactions,⁸ and new allenyl bonding modes in the binuclear com-

plexes $\text{M}_2(\text{CO})_6(\mu\text{-PPh}_2)\{\mu\text{-}\eta^1, \eta^2_{\alpha, \beta}\text{-C(Ph)=C=CH}_2\}$ (M = Ru, Os)⁸ and $\text{Pd}_2(\text{PPh}_3)_2(\mu\text{-Cl})(\mu\text{-}\eta^3\text{-C(H)=C=CH}_2)$.⁹

Herein, we report new reaction pathways for the allenyl ligand in $\text{Ru}_2(\text{CO})_6(\mu\text{-PPh}_2)\{\mu\text{-}\eta^1, \eta^2_{\alpha, \beta}\text{-C(Ph)=C=CPh}_2\}$ (**1**)¹⁰ including (i) a transformation of the $\mu\text{-}\eta^1, \eta^2_{\alpha, \beta}$ -allenyl ligand into a terminal η^1 -metalloallene via displacement of the coordinated $\text{C}_\alpha\text{-C}_\beta$ double bond and (ii) a dppm-induced migratory insertion-elimination sequence for an allenyl ligand. The interconversion of terminal and bridging allenyl ligands has no literature precedent and there is only a single report of the reactivity of binuclear allenyl complexes with diphosphines.⁸

We have previously detailed the reactivity of $\text{Ru}_2(\text{CO})_6(\mu\text{-PPh}_2)\{\mu\text{-}\eta^1, \eta^2_{\beta, \gamma}\text{-C(Ph)=C=CH}_2\}$ (**5**) toward mono-⁴ and bidentate⁸ phosphines. Although closely related, **1** and **5** differ structurally in that the π -coordinated allenyl ligand in **1** is attached via the $\text{C}_\alpha\text{-C}_\beta$ bond and by the $\text{C}_\beta\text{-C}_\gamma$ bond in **5**. We have initiated the current study in an effort to determine how the bonding mode of the allenyl ligand impacts on chemical behavior.

Stirring a room temperature *n*-heptane solution of **1** (0.20 g, 0.24 mmol) with dppm (0.090 g, 0.23 mmol) for 3 h afforded an orange precipitate which, on recrystallization, gave $\text{Ru}_2(\text{CO})_4(\mu\text{-PPh}_2)(\mu\text{-dppm})\{\mu\text{-}\eta^1, \eta^2\text{-C(O)C(Ph)=C=CPh}_2\}$ (**2**) in 80% yield.¹¹ Under similar conditions the reaction of **1** with dppe afforded $\text{Ru}_2(\text{CO})_5(\mu\text{-PPh}_2)(\eta^2\text{-dppe})\{\eta^1\text{-C(Ph)=C=CPh}_2\}$ (**3**) as the sole product (71% yield) after chromatographic workup.¹² In each case reaction monitoring by IR spectroscopy showed only

* Authors to whom correspondence should be addressed.

[†] Steacie Institute.

[‡] GWC2.

[Ⓢ] Abstract published in *Advance ACS Abstracts*, January 1, 1997.

(1) For recent comprehensive reviews see: (a) Wojcicki, A. *New J. Chem.* **1994**, *18*, 61. (b) Doherty, S.; Corrigan, J. F.; Carty, A. J.; Sappa, E. *Adv. Organomet. Chem.* **1995**, *37*, 39.

(2) (a) Huang, T.-M.; Chen, J.-T.; Lee, G.-H.; Wang, Y. *J. Am. Chem. Soc.* **1993**, *115*, 1170. (b) Blosser, P. W.; Schimpff, D. G.; Gallucci, J. C.; Wojcicki, A. *Organometallics* **1993**, *12*, 1993. (c) Huang, T.-M.; Hsu, R.-H.; Yang, C.-S.; Chen, J.-T.; Lee, G.-H.; Wang, Y. *Organometallics* **1994**, *13*, 3657.

(3) See Scheme 1 for the designation of C_α , C_β , and C_γ .

(4) Breckenridge, S. M.; Taylor, N. J.; Carty, A. J. *Organometallics* **1991**, *10*, 837.

(5) (a) Baize, M. W.; Plantevin, V.; Gallucci, J. C.; Wojcicki, A. *Inorg. Chim. Acta* **1995**, *235*, 1. (b) Baize, M. W.; Blosser, P. W.; Plantevin, V.; Schimpff, D. G.; Gallucci, J. C.; Wojcicki, A. *Organometallics* **1996**, *15*, 164.

(6) (a) Shu, H.-G.; Shiu, L.-H.; Wang, S.-H.; Wang, S.-L.; Lee, G.-H.; Peng, S.-M.; Liu, R.-S. *J. Am. Chem. Soc.* **1996**, *118*, 530. (b) Su, C.-C.; Chen, J.-T.; Lee, G.-H.; Wang, Y. *J. Am. Chem. Soc.* **1994**, *116*, 4999. (c) Plantevin, V.; Blosser, P. W.; Gallucci, J. C.; Wojcicki, A. *Organometallics* **1994**, *13*, 3651.

(7) Ogoshi, S.; Fukunishi, Y.; Tsutsumi, K.; Kurosawa, H. *J. Chem. Soc., Chem. Commun.* **1995**, 2485.

(8) Carleton, N.; Corrigan, J. F.; Doherty, S.; Pixner, R. Sun, Y.; Taylor, N. J.; Carty, A. J. *Organometallics* **1994**, *13*, 4179.

(9) Ogoshi, S.; Tsutsumi, K.; Ooi, M.; Kurosawa, H. *J. Am. Chem. Soc.* **1995**, *117*, 10415.

(10) Nucciarone, D.; Taylor, N. J.; Carty, A. J. *Organometallics* **1986**, *5*, 1179.

(11) Spectroscopic data for **2**: IR (CH_2Cl_2) $\nu(\text{CO})/\text{cm}^{-1}$, 2025 w, 2010 s, 1967 m, 1961 sh; ¹H NMR (CDCl_3) δ 7.61–5.82 (m, 45H, Ph), 4.39 (dd, 1H, Ph_2PCH_2), 3.93 (m, 1H, Ph_2PCH_2); ³¹P{¹H} NMR (CDCl_3) δ 129.3 (dd, $J_{\text{P}\mu\text{P}} = 23.2$ Hz, $J_{\text{P}\mu\text{P}} = 17.5$ Hz, $\mu\text{-P}$), 29.3 (dd, $J_{\text{P}\mu\text{P}} = 139.0$ Hz, $J_{\text{P}\mu\text{P}} = 17.5$ Hz, dppm), 2.5 (dd, $J_{\text{P}\mu\text{P}} = 139.0$ Hz, $J_{\text{P}\mu\text{P}} = 23.2$ Hz, dppm). Anal. Calc for $\text{C}_{63}\text{H}_{47}\text{O}_5\text{P}_3\text{Ru}_2$: C, 64.17; H, 4.02. Found: C, 63.98; H, 4.22.

(12) Spectroscopic data for **3**: IR (C_6H_{12}) $\nu(\text{CO})/\text{cm}^{-1}$, 2005 sh, 1992 s, 1980 sh, 1946 m, 1923 m; ¹H NMR (CDCl_3) δ 7.81–6.71 (m, 45H, Ph), 2.10 (dd, $J_{\text{PH}} = 20.0$ Hz, $J_{\text{HH}} = 2.7$ Hz, 2H, Ph_2PCH_2), 2.06 (t, $J_{\text{PH}} = 5.2$ Hz, $J_{\text{HH}} = 5.2$ Hz, 2H, Ph_2PCH_2); ³¹P{¹H} NMR (CDCl_3) δ 107.2 (dd, $J_{\text{P}\mu\text{P}} = 132.0$ Hz, $J_{\text{P}\mu\text{P}} = 14.0$ Hz, $\mu\text{-P}$), 63.0 (dd, $J_{\text{P}\mu\text{P}} = 132.0$ Hz, $J_{\text{P}\mu\text{P}} = 14.0$ Hz, dppe), 58.0 (dd, $J_{\text{P}\mu\text{P}} = 14.0$ Hz, $J_{\text{P}\mu\text{P}} = 14.0$ Hz, dppe). Anal. Calc for $\text{C}_{64}\text{H}_{49}\text{O}_5\text{P}_3\text{Ru}_2$: C, 64.43; H, 4.14. Found: C, 63.80; H, 4.19.

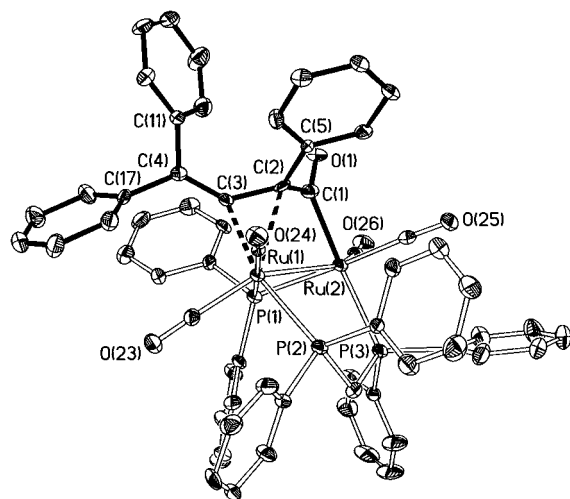


Figure 1. Molecular structure of $\text{Ru}_2(\text{CO})_4(\mu\text{-PPh}_2)(\mu\text{-dppm})\{\mu\text{-}\eta^1, \eta^2\text{-C(O)C(Ph)=C=CPh}_2\}$ (**2**) with the non-hydrogen atom-labeling scheme. Important bond lengths and angles not mentioned in the text are as follows: C(1)–C(2) 1.510(14), C(1)–O(1) 1.213(12), Ru(1)–Ru(2) 2.9697(12) Å; Ru(2)–C(1)–O(1) 130.1(8), O(1)–C(1)–C(2) 122.9(9), C(1)–C(2)–C(3) 118.5(9), P(1)–Ru(1)–P(2) 99.26(9), P(1)–Ru(2)–P(3) 94.93(9), Ru(1)–P(1)–Ru(2) 77.56(8)°.

the formation of the final isolated product. The ^{31}P NMR spectra for **2** and **3** each showed three distinct sets of resonances indicating incorporation of the diphosphine ligand. However, their disparate chemical shifts and J values suggested different reaction pathways for these phosphines. Single-crystal X-ray studies were therefore carried out on **2**¹³ and **3**¹⁴ to elucidate their structures (Figure 1).

The most notable feature of **2** is the acylallenyl ligand, formally derived from the insertion of CO into the $\text{Ru}-\text{C}_\alpha$ bond of **1**. The resulting ligand is σ -bound to Ru(2) through the carbonyl carbon (Ru(2)–C(1) = 2.053(10) Å) and attached to Ru(1) via an η^2 interaction with $\text{C}_\alpha-\text{C}_\beta$ (Ru(1)–C(2) = 2.374(10) Å, Ru(1)–C(3) = 2.105(10) Å). The incorporation of a CO group in **2** effects a significant elongation of the $\text{C}_\alpha-\text{C}_\beta$ bond¹⁰ (C(2)–C(3) = 1.438(14) Å vs 1.382(11) Å in **1**) while the outer uncoordinated $\text{C}_\beta-\text{C}_\gamma$ bond remains essentially unchanged (C(3)–C(4) = 1.340(14) Å). The retention of allenic character in the new fragment is highlighted by

(13) Crystal data for **2**· $\text{CH}_2\text{Cl}_2 \cdot 0.5\text{C}_6\text{H}_{14}$: $\text{C}_{67}\text{H}_{56}\text{Cl}_2\text{O}_5\text{P}_3\text{Ru}_2$, $M = 1307.1$; triclinic, space group $P\bar{1}$; $a = 11.7781(10)$, $b = 14.1291(11)$, $c = 19.130(2)$ Å; $\alpha = 89.499(2)$, $\beta = 73.406(2)$, $\gamma = 67.870(2)$ °; $V = 2808.6(4)$ Å³, $Z = 2$, $T = 160$ K, $D_c = 1.546$ g cm^{-3} , $F(000) = 1330$, $\lambda = 0.710$ 73 Å, $\mu(\text{Mo K}\alpha) = 0.771$ mm^{-1} . Intensity data were collected on a crystal of dimensions $0.16 \times 0.08 \times 0.07$ mm mounted on a Siemens SMART CCD area detector diffractometer. Of 28 920 reflections measured ($\theta_{\text{max}} = 25.0^\circ$), 9857 were unique ($R_{\text{int}} = 0.108$). Semi-empirical absorption corrections were applied (transmission 0.605–0.986). The structure was solved by Patterson synthesis and refinement based on F^2 with statistical-based weighting scheme, anisotropic displacement parameters, constrained isotropic H atoms, and restraints on possibly disordered (unresolved) n -hexane solvent; final $wR2 = \{\sum[w(F_o^2 - F_c^2)]^2 / \sum[w(F_o^2)]^2\}^{1/2} = 0.223$ for all data. Conventional $R = 0.100$ on F values of 7378 reflections having $F_o^2 > 2\sigma(F_o^2)$, $S = 1.26$ on F^2 for all data, 713 refined parameters and 39 restraints.

(14) Crystal data for **3**· CH_2Cl_2 : $\text{C}_{65}\text{H}_{51}\text{Cl}_2\text{O}_5\text{P}_3\text{Ru}_2$, $M = 1278.0$; monoclinic, space group $P2_1/n$; $a = 13.923(2)$, $b = 19.567(3)$, $c = 21.089(3)$ Å; $\beta = 94.96(2)$ °; $V = 5723.7(14)$ Å³, $Z = 4$, $T = 200$ K, $D_c = 1.483$ g cm^{-3} , $F(000) = 2592$, $\lambda = 0.710$ 73 Å, $\mu(\text{Mo K}\alpha) = 7.55$ cm^{-1} . Intensity data were collected on a crystal of dimensions $0.30 \times 0.40 \times 0.74 \times 0.65$ mm mounted on a Siemens R3m/V diffractometer by the ω scan method ($2\theta < 50^\circ$). An absorption correction (face-indexed numerical) was applied (transmission 0.729–0.817). Of 10 116 reflections measured, 8255 were considered observed [$F > 6.0\sigma(F)$]. The structure was solved (Patterson, Fourier methods) and refined (full-matrix least-squares) using the Siemens SHELXTL PLUS program, giving final R and R_w values (based on F_o^2) of 0.0302 and 0.0334, respectively.

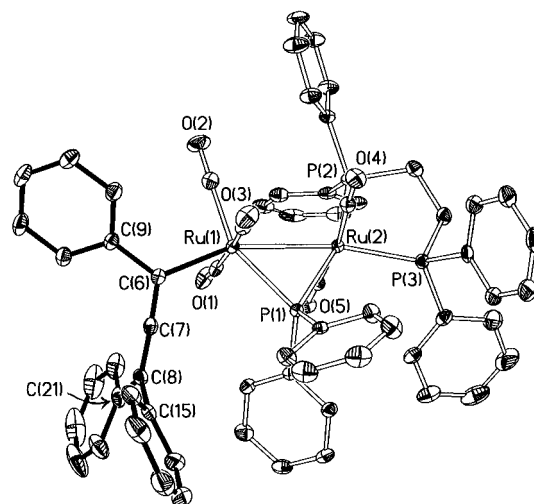


Figure 2. Molecular structure of $\text{Ru}_2(\text{CO})_5(\mu\text{-PPh}_2)(\eta^2\text{-dppe})\{\eta^1\text{-C(Ph)=C=CPh}_2\}$ (**3**) with the non-hydrogen atom-labeling scheme. Important bond lengths and angles not mentioned in the text are as follows: Ru(1)–Ru(2) 2.926(1) Å; Ru(1)–C(6)–C(7) 120.6(2), P(2)–Ru(2)–P(3) 85.8(1), C(6)–Ru(1)–Ru(2) 159.2(1), Ru(1)–P(1)–Ru(2) 76.5(1)°.

the dihedral angle of 82.4° between the planes defined by C(4)–C(11)–C(17) and C(2)–C(1)–C(5). However, the η^2 -coordination of C(2)–C(3) and the steric congestion imposed by the bulky phenyl substituents on P(1) and P(2) creates a further distortion from linearity in the allenic backbone of **2** (C(2)–C(3)–C(4) = 136.5(9)°).

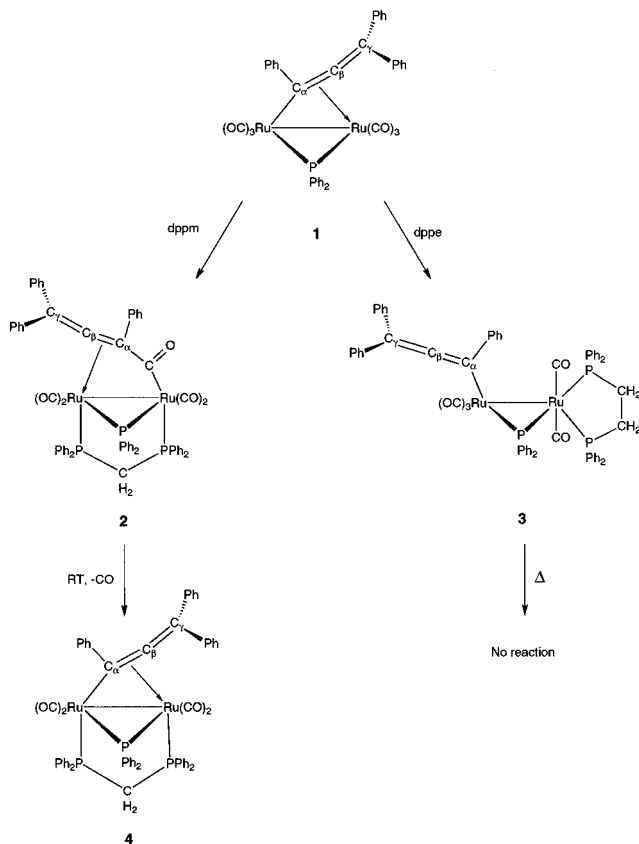
The molecular structure of **3** (Figure 2) revealed a novel η^1 -coordination mode for the allenyl ligand. Thus, in contrast to **2**, the η^1 -allenyl linkage to the metal in **3** remains intact, although a significant elongation of the $\text{Ru}-\text{C}_\sigma$ bond results (Ru(1)–C(6) = 2.158(3) Å; cf. 2.101(8) Å in **1**). Equally, the displacement of the π -coordinated $\text{C}_\alpha-\text{C}_\beta$ bond in precursor **1** causes a contraction in allenic bond lengths (C(6)–C(7) = 1.293(5), C(7)–C(8) = 1.328(5) Å) to give values typical for terminal allenyl complexes.^{2c,18} The near-linear hydrocarbyl backbone in **3** (C(6)–C(7)–C(8) = 175.5(3) Å) and the dihedral angle of 83.4° formed between the Ru(1)–C(6)–C(9) and C(15)–C(8)–C(21) planes is consistent with a metalloallene designation. In the formation of **3**, the loss of a CO ligand and slippage of the $\mu\text{-}\eta^1, \eta^2$ -coordinated allenyl to η^1 -mode generates two vacant sites on Ru(2) to which the dppe ligand becomes coordinated as a chelating group with one arm binding *trans* (P(1)–Ru(2)–P(2) = 160.8(1)°) and one *cis* (P(1)–Ru(2)–P(3) = 94.93(9)°) to the phosphido bridge, consistent with $J_{\text{P}\mu\text{P}_{\text{dppe}}}$ couplings of 132.0 and 14.0 Hz, respectively.

The conversion of a $\mu\text{-}\eta^1, \eta^2$ -bound allenyl ligand into a terminal metalloallene is unprecedented in polynuclear chemistry. However, Wojcicki and co-workers have demonstrated the conversion of an η^3 -propargyl/allenyl ligand to an η^1 arrangement in the treatment of the platinum cation $[(\text{Ph}_3\text{P})_2\text{Pt}(\eta^3\text{-CH}_2\text{CCPh})]^+$ with excess PMe_3 or CO .^{2b}

Room-temperature solutions of **2** readily lose CO over 24 h to afford $\text{Ru}_2(\text{CO})_4(\mu\text{-PPh}_2)(\mu\text{-dppm})\{\mu\text{-}\eta^1, \eta^2\text{-C(Ph)=C=CPh}_2\}$ (**4**) (Scheme 1), a transformation which also occurs quantitatively and more rapidly at elevated

(15) (a) Wouters, J. M. A.; Klein, R. A.; Elsevier, C. J.; Zoutberg, M. C.; Stam, C. H. *Organometallics* **1993**, *12*, 3864. (b) Wouters, J. M. A.; Klein, R. A.; Elsevier, C. J.; Haming, L.; Stam, C. H. *Organometallics* **1994**, *13*, 4586. (c) Blosser, P. W.; Gallucci, J. C.; Wojcicki, A. *J. Am. Chem. Soc.* **1993**, *115*, 2994.

Scheme 1



temperatures. The ^{31}P NMR spectrum is consistent with the retention of a phosphido bridge and a bridging diphosphine ligand.¹⁶ The structure (Figure 3)¹⁷ shows an $\text{Ru}_2(\text{CO})_4(\mu\text{-PPh}_2)(\mu\text{-dppm})$ framework, similar to that found in **2**. In this case however, the acylallenyl ligand has undergone elimination of one molecule of CO to regenerate the $\mu\text{-}\eta^1, \eta^2_{\alpha, \beta}$ -allenyl ligand present in **1**. Thus the C_3 fragment is σ -bound via C(5) to Ru(1) (2.082(4) Å) and linked to Ru(2) via a π -interaction with the $\text{C}_\alpha\text{-C}_\beta$ double bond (Ru(2)–C(5) = 2.344(3), Ru(2)–C(6) = 2.135(3) Å). The structural parameters of the hydrocarbyl group are closely related to those found in **1**.¹⁰

Although CO insertion/elimination sequences are commonplace for mononuclear σ -bonded organometallics, this is the first example of such a stepwise transformation on a binuclear allenyl complex. Acylallenyl ligands of mononuclear platinum and palladium complexes have been reported as intermediates in the preparation of furanoylmetal compounds^{15a} as well as during the template synthesis of heterobimetallics from mono-

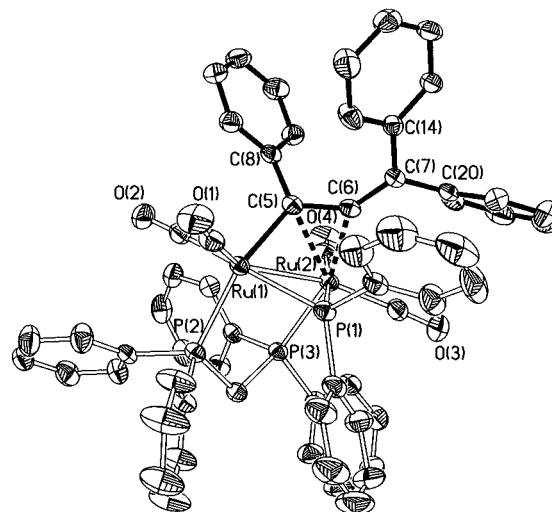


Figure 3. Molecular structure of $\text{Ru}_2(\text{CO})_4(\mu\text{-PPh}_2)(\mu\text{-dppm})\{\mu\text{-}\eta^1, \eta^2_{\alpha, \beta}\text{-C}(\text{Ph})=\text{C}=\text{CPh}_2\}$ (**4**) with the non-hydrogen atom-labeling scheme. Important bond lengths and angles not mentioned in the text are as follows: Ru(1)–Ru(2) 2.819(1), C(5)–C(6) 1.402(6), C(6)–C(7) 1.341(5) Å; C(5)–C(6)–C(7) 140.2(3), Ru(1)–C(5)–C(6) 124.9(3), Ru(2)–C(6)–C(7) 139.3(3), P(1)–Ru(1)–P(2) 90.4(1), P(1)–Ru(2)–P(3) 94.7(1), Ru(1)–P(1)–Ru(2) 72.9(1)°.

nuclear η^1 -propargyl complexes.¹⁸ Wojcicki and co-workers have described the binuclear complex $\text{CpRu}(\text{CO})(\text{CO})\text{Fe}(\text{CO})_3\{\mu\text{-}\eta^3, \eta^2\text{-C}(\text{O})\text{C}(\text{Ph})=\text{C}=\text{CH}_2\}$ which features a 5-electron donor acylallenyl ligand in which both allenyl C=C bonds are π -coordinated to a metal center.¹⁹ In contrast to **2** however, no acyl ligand decarbonylation was observed on reaction with dppm.

The reaction of **1** with dppm is in sharp contrast to that reported for $\text{Ru}_2(\text{CO})_6(\mu\text{-PPh}_2)\{\mu\text{-}\eta^1, \eta^2_{\beta, \gamma}\text{-C}(\text{Ph})=\text{C}=\text{CH}_2\}$ in which the phosphido, allenyl, and carbonyl groups couple together.⁸ In the latter case although the intermediacy of an allenyl analogue $\text{Ru}_2(\text{CO})_4(\mu\text{-PPh}_2)(\mu\text{-dppm})\{\mu\text{-}\eta^1, \eta^2\text{-C}(\text{O})\text{C}(\text{Ph})=\text{C}=\text{CH}_2\}$ of **2** in the formation of the final coupled product might be expected, this was not verified spectroscopically. Clearly the nature of the diphosphine influences the hapticity of the hydrocarbyl fragment. The preference of dppe for a chelate interaction with the metal in **3** is key in displacing the allenyl from the η^2 -coordinated metal site and is likely the result of steric crowding at Ru(2). The attachment of the dppm ligand in **2** and **4** in a bridging position facilitates bonding of the hydrocarbyl group to both metal atoms.

The present study illustrates the versatility of the allenyl ligand and its adaptability in coordinating to metal centers. Control over the hapticity of this C_3 fragment may be achieved through judicious selection of the ligand environment.

Acknowledgment. We gratefully acknowledge support from the Natural Sciences and Engineering Research Council (NSERC) and the National Research Council of Canada (to A.J.C.) and the EPSRC for funding for a diffractometer (to W.C.).

Supporting Information Available: For **2–4** details of the structure determination (Tables S1, S6, and S11), non-

(16) Spectroscopic data for **4**: IR (C_6H_{12}) $\nu(\text{CO})/\text{cm}^{-1}$ 2024 w, 2010 s, 1996 m; ^1H NMR (CDCl_3) δ 7.51–5.82 (m, 45H, Ph), 4.05 (m, 1H, $\text{Ph}_2\text{PC}_2\text{H}_2$), 3.31 (m, 1H, $\text{Ph}_2\text{PC}_2\text{H}_2$); $^{31}\text{P}\{^1\text{H}\}$ NMR (CDCl_3) δ 122.2 (dd, $J_{\text{P}(\mu\text{P})\text{P}(\text{dppm})} = 37.0$ Hz, $J_{\text{P}(\mu\text{P})\text{P}(\text{dppm})} = 23.0$ Hz, $\mu\text{-P}$), 23.5 (dd, $J_{\text{P}(\text{dppm})\text{P}(\text{dppm})} = 92.0$ Hz, $J_{\text{P}(\mu\text{P})\text{P}(\text{dppm})} = 23.0$ Hz, dppm), 13.5 (dd, $J_{\text{P}(\text{dppm})\text{P}(\text{dppm})} = 92.0$ Hz, $J_{\text{P}(\mu\text{P})\text{P}(\text{dppm})} = 37.0$ Hz, dppm). Anal. Calc for $\text{C}_{62}\text{H}_{47}\text{O}_4\text{P}_3\text{Ru}_2$: C, 64.69; H, 4.12. Found: C, 63.98; H, 4.22.

(17) Crystal data for **4**· C_6H_6 : $\text{C}_{68}\text{H}_{53}\text{O}_4\text{P}_3\text{Ru}_2$, $M = 1229.2$; monoclinic, space group $C2/c$; $a = 40.684(6)$, $b = 12.305(2)$, $c = 23.972(3)$ Å; $\beta = 102.90(2)^\circ$, $V = 11698(2)$ Å³, $Z = 8$, $T = 294$ K, $D_c = 1.396$ g cm⁻³, $F(000) = 5008$, $\lambda = 0.710$ 73 Å, $\mu(\text{Mo K}\alpha) = 6.47$ cm⁻¹. Intensity data were collected on a crystal of dimensions $0.78 \times 0.56 \times 0.68 \times 0.92 \times 0.81$ mm mounted on a Siemens R3m/V diffractometer by the ω scan method ($2\theta < 50^\circ$). An absorption correction (face-indexed numerical) was applied (transmission 0.665–0.730). Of 10 328 reflections measured, 8390 were considered observed [$F > 6.0\sigma(F)$]. The structure was solved and refined as for **3**, giving final R and R_w values (based on F_o^2) of 0.0316 and 0.0361 respectively.

(18) Wojcicki, A.; Schuchart, C. E. *Coord. Chem. Rev.* **1990**, *105*, 35.

(19) (a) Schuchart, C. E.; Young, G. H.; Wojcicki, A.; Calligaris, M.; Nardin, G. *Organometallics* **1990**, *9*, 2417. (b) Schuchart, C. E.; Wojcicki, A.; Calligaris, M.; Faleschini, P.; Nardin, G. *Organometallics* **1994**, *13*, 1999.

hydrogen atomic positional and U parameters (Tables S2, S7, and S12), bond distances and angles (Tables S3, S8, and S13), anisotropic displacement parameters (Tables S4, S9, and S14), and hydrogen atom parameters (Tables S5, S10, and S15) (34

pages). Ordering information is given on any current mast-head page. Observed and calculated structure factor tables are available from the authors upon request.

OM9607208